UC San Diego
UC San Diego Previously Published Works

Title

Model reduction and stochastic analysis of the histone modification circuit**This work was supported by NIH/NIBIB Grant Number R01EB024591 in part by NSF Collaborative Research grant MCB-2027949 and by the DoD Newton Award for Transformative Ideas du...

Permalink

Authors

Bruno, Simone
Williams, Ruth J
Del Vecchio, Domitilla

Publication Date

2022-07-15

DOI

Copyright Information

Peer reviewed

Model reduction and stochastic analysis
of the histone modification circuit

Simone Bruno[1] and Ruth J. Williams[2] and Domitilla Del Vecchio[1]

Abstract—**Epigenetic cell memory (ECM), the inheritance of gene expression patterns without changes in genetic sequence, is a critical property of multi-cellular organisms. Chromatin state, as dictated by histone covalent modifications, has recently appeared as a mediator of ECM. In this paper, we conduct a stochastic analysis of the histone modification circuit that controls chromatin state to determine key biological parameters that affect ECM. Specifically, we derive a one-dimensional Markov chain model of the circuit and analytically evaluate both the stationary probability distribution of chromatin state and the mean time to switch between active and repressed chromatin states. We then validate our analytical findings using stochastic simulations of the original higher dimensional circuit reaction model. Our analysis shows that as the speed of basal decay of histone modifications decreases compared to the speed of autocatalysis, the stationary probability distribution becomes bimodal and increasingly concentrated about the active and repressed chromatin states. Accordingly, the switching time between active and repressed chromatin states becomes larger. These results indicate that time scale separation among key constituent processes of the histone modification circuit controls ECM.**

I. INTRODUCTION

Epigenetic cell memory (ECM), the inheritance of gene expression patterns without changes in genetic sequence, is the property according to which cells with identical genomes can maintain distinct identities for the life-time of a multi-cellular organism. This enables co-existence of different cell states that do not spontaneously interconvert among each other despite the influence of noise. The ECM question has been addressed mostly in the context of gene regulatory network (GRN) models and by determining topologies and parameters that allow multi-stability [1]–[6]. More recently, it was noted that these models do not account for chromatin state, as determined by covalent modifications to histones and DNA [7]. Yet, the state of chromatin has

[1]Department of Mechanical Engineering, Massachusetts Institute of Technology, 77 Massachusetts Avenue, Cambridge, MA 02139. Emails: (`sbruno,ddv`)`@mit.edu`
[2]Department of Mathematics, University of California, San Diego, 9500 Gilman Drive, La Jolla CA 92093-0112. Email: `rjwilliams@ucsd.edu`

appeared a key mediator of long-term memory of gene states [8].

In this paper, we analyze the dynamics of a ubiquitous circuit motif among histone modifications [9] and determine how its kinetic parameters affect the duration of memory of chromatin states. To this end, we first show that our deterministic model is a *singular singularly perturbed system* [10] and apply a proper reduction method to obtain a one-dimensional reduced model suitable for analytical investigation. Then, we analytically evaluate the stationary distribution of the corresponding one-dimensional Markov chain by applying detailed balance [11] and determine the parameter conditions that give a bimodal distribution with peaks at the active and repressed chromatin states. We then derive an expression for the *time to memory loss*, defined as the mean value of the earliest time the active state reaches the repressed state and *viceversa* by first step analysis [12]. We finally validate the analytical findings by conducting a computational study of the original circuit reaction model using Gillespie's Stochastic Simulation Algorithm (SSA) [13]. Research on the dynamics of histone modifications conducted in the past decade has considered bistability as a model property embodying ECM [9], [14]–[19]. However, there has not been any investigation on the key determinants of the temporal duration of memory, which is the question addressed in this paper.

This paper is organized as follows. In Section II, we describe the molecular reactions constituting the histone modification circuit. In Section III, we present the deterministic model reduction approach to obtain the one-dimensional reduced model. Then, in Section IV we analytically investigate the properties of the resulting one-dimensional Markov chain and in Section V we use stochastic simulation of the original reaction model to validate the analytical findings. Conclusive remarks are presented in Section VI.

II. HISTONE MODIFICATION CIRCUIT REACTION MODEL

In this paper we focus on the reaction model of the histone modification circuit shown in Fig. 1(a). It includes H3K9 methylation and H3K4 methylation/ acetylation and it is developed by exploiting the detailed
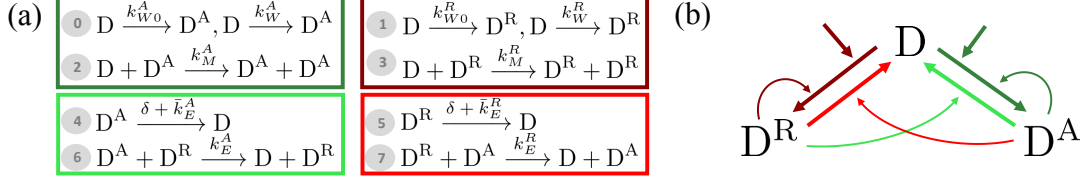
Fig. 1: Histone modification circuit: reactions and diagram. (a) Reaction list of the original histone modification circuit. A number, referred in the main text, is associated to each reaction. Specifically, reactions ⓪ and ① describe *de novo* establishment, ② and ③ describe self-maintenance, ④ and ⑤ represent basal erasure and ⑥ and ⑦ represent recruited erasure. The different colored boxes delimit the sets of reactions associated to the establishment (dark colors) and erasure (light colors) of D^A (green) and D^R (red). Here, to model the establishment and erasure of the histone modifications we exploit the one-step enzymatic reaction models [20]. (b) Diagram of the histone modification circuit, in which each arrow corresponds to the reaction withing the box of the same color in (a).

characterization of the molecular properties of these modifications done in the past years [21]–[25]. This model has the nucleosome with DNA wrapped around it, D, as basic unit that can be modified either with H3K4 methylation/acetylation, D^A, or H3K9 methylation, D^R. H3K4 methylation/acetylation are associated with active chromatin state ([8], Chapter 3 and [23]), while H3K9 methylation (H3K9me1/2/3) is associated with repressed chromatin state [26]. Now, let us give a concise summary of the key molecular mechanisms characterizing the histone modification circuit. H3K4 methylation/acetylation can be *de novo* established by the action of writer enzymes (reactions ⓪ in Fig. 1(a)) and can be maintained through a read-write process in which D^A can recruit writers of the same modification [8] (reactions ② in Fig. 1(a)). With similar processes, H3K9 methylation can be *de novo* established (① in Fig. 1(a)) and maintained (③ in Fig. 1(a)). These modifications can both be passively removed through dilution due to DNA replication or through non-specific de-methylation/ de-acetylation ([8], Chapter 22) (reactions ④, ⑤ in Fig. 1(a)), and actively removed by the action of eraser enzymes recruited by the opposite modifications (reactions ⑥ and ⑦ in Fig. 1(a)). Then, each histone modification creates a positive autoregulation loop and inhibits the other one. The reactions describing the histone modification circuit are listed in Fig. 1(a) and the corresponding circuit is represented in Fig. 1(b).

We next derive the associated ordinary differential equation (ODE) model. In particular, we assume that D_{tot}, that is, the number of total modifiable units, is sufficiently large such that the variables n_{D^A}, n_{D^R} and n_D can be considered real-valued. This allows us to write the ODEs in terms of the fractions $\bar{D}^A = n_{D^A}/D_{tot}$, $\bar{D}^R = n_{D^R}/D_{tot}$ and $\bar{D} = n_D/D_{tot}$. We further introduce the normalized time $\tau = tk_M^A D_{tot}$, in which $D_{tot} = D_{tot}/\Omega$ and Ω is the reaction volume; the normalized inputs $\bar{u}_A = u_{A0} + u_A$ with $u_{A0} = k_{W0}^A/(k_M^A D_{tot})$, $u_A = k_W^A/(k_M^A D_{tot})$, $\bar{u}_R = u_{R0} + u_R$ with $u_{R0} = k_{W0}^R/(k_M^A D_{tot})$ and $u_R = k_W^R/(k_M^A D_{tot})$

and the non-dimensional parameter $\alpha = k_M^R/k_M^A$. Furthermore, let us also introduce

$$\varepsilon = \frac{\delta + \bar{k}_E^A}{k_M^A D_{tot}}, \quad \varepsilon' = \frac{k_E^A}{k_M^A}, \quad \mu = \frac{k_E^R}{k_E^A}. \quad (1)$$

and we let $(\delta + \bar{k}_E^R)/(\delta + \bar{k}_E^A) = b\mu$ with $b = O(1)$. This implies that μ quantifies the asymmetry between the erasure rates of repressive and activating marks. Furthermore, since $(\delta + \bar{k}_E^R)/(k_M^A D_{tot}) = b\varepsilon\mu$ and $k_E^R/k_M^A = \mu\varepsilon'$, it implies that ε is a parameter that scales the ratio between the basal erasure rate of each histone modification and the rate at which they are copied and ε' is a parameter that scales the ratio between the recruited erasure rate of each modification and the rate at which they are copied. Then, the ODEs describing the histone modification circuit can be written as follows:

$$\frac{d\bar{D}^A}{d\tau} = (\bar{u}_A + \bar{D}^A)\bar{D} - (\varepsilon + \varepsilon'\bar{D}^R)\bar{D}^A$$
$$\frac{d\bar{D}^R}{d\tau} = (\bar{u}_R + \alpha\bar{D}^R)\bar{D} - \mu(b\varepsilon + \varepsilon'\bar{D}^A)\bar{D}^R \quad (2)$$
$$\frac{d\bar{D}}{d\tau} = \left(\mu\left(b\varepsilon + \varepsilon'\bar{D}^A\right)\bar{D}^R + \left(\varepsilon + \varepsilon'\bar{D}^R\right)\bar{D}^A\right)$$
$$- (\bar{u}_R + \alpha\bar{D}^R + \bar{u}_A + \bar{D}^A)\bar{D}$$

with initial conditions such that $\bar{D} + \bar{D}^A + \bar{D}^R = 1$.

III. MODEL REDUCTION

In this section, we reduce the system (2) to a one-dimensional model by exploiting time scale separation between reactions. Specifically, we let $\varepsilon = c\varepsilon'$ with $c = O(1)$ and consider ε' as the small non-dimensional parameter encapsulating the time scale separation between autocatalytic reactions (faster) and erasure reactions (slower). This assumption is consistent with recent experimental data that suggest that the natural erasure of histone modifications is a slow process [27]. It further allows us to obtain an ε-dependent one-dimensional system whose properties as function of ε can be analytically determined. We then show computationally that

the analytically obtained trends with ε are mirrored by the original system where this time scale separation may not hold.

We first introduce the model reduction method considered [10], and then we apply it to the histone modification circuit model (2). In particular, we will show that with ε' as small parameter, the system model in equations (2) belongs to the class of singular singularly perturbed problems, which we introduce in the next section.

A. Model reduction approach

Given a general dynamical system $\frac{dx}{dt} = f(x,t)$ with $x \in \mathbb{R}^n$, let us define a smooth surface S in $\mathbb{R}^n \times \mathbb{R}$ as integral manifold of the system if any trajectory of the system that has at least one point in common with S lies entirely on S [28], [29]. Now, let us consider the system:

$$\begin{aligned} \varepsilon' \dot{x} &= f_1(x, y_2, t, \varepsilon') \\ \varepsilon' \dot{y}_2 &= f_2(x, y_2, t, \varepsilon') \end{aligned} \quad (3)$$

with $x \in \mathbb{R}^m$ and $y_2 \in \mathbb{R}^n$ and the matrix $A(x, y_2, t, \varepsilon')$ given by

$$A(x, y_2, t, \varepsilon') = \begin{pmatrix} \frac{\partial f_1}{\partial x} & \frac{\partial f_1}{\partial y_2} \\ \frac{\partial f_2}{\partial x} & \frac{\partial f_2}{\partial y_2} \end{pmatrix} = \begin{pmatrix} f_{1x} & f_{1y_2} \\ f_{2x} & f_{2y_2} \end{pmatrix} \quad (4)$$

If $A(x, y_2, t, 0)$ is singular on some subspace of $\mathbb{R}^m \times \mathbb{R}^n \times \mathbb{R}$, system (3) is called a *singular singularly perturbed system* [10]. Now, let us consider the following conditions [10]:

- **C1:** $f_2(x, y_2, t, 0) = 0$ has a smooth isolated root $y_2 = \phi(x, t)$ with $x \in \mathbb{R}^m$, $t \in \mathbb{R}$ and $f_2(x, \phi(x, t), t, 0) = 0$;
- **C2:** the matrix $A(x, y_2{=}\phi(x, t), t, \varepsilon'{=}0)$ has a m-dimensional kernel and m corresponding linearly independent eigenvectors, and the matrix

$$B(x, \phi(x, t), t, 0) = \frac{\partial f_2(x, \phi(x, t), t, 0)}{\partial y_2} \quad (5)$$

  has n eigenvalues $\lambda_i(x, t)$ such that $Re\lambda_i(x, t) \leq -2\alpha$, with $\alpha > 0$;
- **C3:** in the domain $\Omega = \{(x, y_2, t, \varepsilon') | x \in \mathbb{R}^m, ||y_2 - \phi(x, t)|| \leq \rho, t \in \mathbb{R}, 0 \leq \varepsilon' \leq \varepsilon'_0\}$ the function f_1 and f_2 and the matrix A are continuously differentiable $(k + 2)$ times, with $k \geq 0$ for some positive ε'_0 and ρ.

Furthermore, let us define the new variables $y_2 = y_1 + \phi(x, t)$ and introduce them in (3), obtaining

$$\begin{aligned} \varepsilon' \dot{x} &= C(x, t)y_1 + F_1(x, y_1, t) + \varepsilon' X(x, y_1, t, \varepsilon') \\ \varepsilon' \dot{y}_1 &= B(x, t)y_1 + F_2(x, y_1, t) + \varepsilon' Y(x, y_1, t, \varepsilon'), \end{aligned} \quad (6)$$

in which

$$\begin{aligned} C(x, t) &= f_{1y_2}(x, \phi(x, t), t, 0), \\ B(x, t) &= f_{2y_2}(x, \phi(x, t), t, 0), \end{aligned}$$

$$\begin{aligned} F_1(x, y_1, t) &= f_1(x, y_1 + \phi(x, t), t, 0) - C(x, t)y_1, \\ F_2(x, y_2, t) &= f_2(x, y_1 + \phi(x, t), t, 0) - B(x, t)y_1, \\ \varepsilon' X(x, y_1, t, \varepsilon') &= f_1(x, y_1 + \phi(x, t), t, \varepsilon') \\ &\quad - f_1(x, y_1 + \phi(x, t), t, 0), \\ \varepsilon' Y(x, y_1, t, \varepsilon') &= f_2(x, y_1 + \phi(x, t), t, \varepsilon') \\ &\quad - f_2(x, y_1 + \phi(x, t), t, 0), \end{aligned} \quad (7)$$

with F_i, $i = 1, 2$, satisfying $||F_i(x, y_1, t)|| = O(||y_1||^2)$ and $\varepsilon'^{-1} F_i(x, \varepsilon' y, t)$ continuous in Ω, with Ω defined in condition **C3** [10]. At this point we can apply Theorem 7.1 from [10], which claims that if conditions **C1** - **C3** are satisfied, then there exists an ε'_1, $0 < \varepsilon'_1 < \varepsilon'_0$, such that, for any $\varepsilon' \in (0, \varepsilon'_1)$, system (6) has a unique slow integral manifold $y_1 = \varepsilon' h(x, t, \varepsilon')$ exponentially attractive and the motion along this manifold is described by the equation:

$$\dot{\bar{x}} = X_1(\bar{x}, t, \varepsilon') \quad (8)$$

with $X_1(\bar{x}, t, \varepsilon') = C(\bar{x}, t)h(\bar{x}, t, \varepsilon') + X(\bar{x}, \varepsilon' h, t, \varepsilon') + \varepsilon'^{-1} F_1(\bar{x}, \varepsilon' h, t)$ and the function $h(x, t, \varepsilon')$ is k times continuously differentiable with respect to x and t [10], [30]. Since for a sufficiently small ε' the slow integral manifold is exponentially attractive, then, for any solution $x(t), y_1(t)$ of (6) with initial conditions $x(t_0) = x_0, y_1(t_0) = y_{10}$ such that $|y_{10} - \varepsilon' h(x_0, t_0, \varepsilon')|$ is sufficiently small, we have a solution of (8) such that

$$x(t) = \bar{x}(t) + \zeta_1(t), \quad y_1(t) = \varepsilon' h(\bar{x}(t), t, \varepsilon') + \zeta_2(t),$$

with $\zeta_i(t) = O(e^{-(\alpha/\varepsilon')(t - t_0)})$, $i = 1, 2$, and $t \geq t_0$ ([10], [31], [32] Chapter 6). This allows us to determine the behavior of the trajectories of the original system near the integral manifold by analyzing the trajectories of the reduced system (8).

As explained in [10], [29], we can determine $h(x, t, \varepsilon')$ by exploiting the change of variable $y = y_1/\varepsilon'$ that allows us to re-write (6) in the standard singular perturbation form:

$$\begin{aligned} \dot{x} &= \tilde{X}(x, y, t, \varepsilon'), \quad x \in \mathbb{R}^m, \ t \in \mathbb{R}, \\ \varepsilon' \dot{y} &= \tilde{Y}(x, y, t, \varepsilon'), \quad y \in \mathbb{R}^n, \end{aligned} \quad (9)$$

in which $\tilde{X}(x, y, t, \varepsilon') = C(x, t)y + \varepsilon'^{-1} F_1(x, \varepsilon' y, t) + X(x, \varepsilon' y, t, \varepsilon')$, $\tilde{Y}(x, y, t, \varepsilon') = B(x, t)y + \varepsilon'^{-1} F_2(x, \varepsilon' y, t) + Y(x, \varepsilon' y, t, \varepsilon')$. Since F_i, $i = 1, 2$, satisfy $||F_i(x, y_1, t)|| = O(||y_1||^2)$ in Ω, then $\varepsilon'^{-1} F_i(x, \varepsilon' y, t)$ are well defined as ε' approaches zero [10]. Then, defining the smooth isolated root of $\tilde{Y}(x, y, t, 0) = 0$ as $y = h_0(x, t)$, it is possible to show that, since conditions **C1** - **C3** are satisfied, the eigenvalues λ_i of the matrix $(\partial \tilde{Y}/\partial y)(x, h_0(x, t), t, 0)$ satisfy the inequality $Re(\lambda_i) \leq -2\alpha$, with $\alpha > 0$. Then, the integral manifold $y = y_1/\varepsilon' = h(x, t, \varepsilon')$ can be calculated as asymptotic expansion in integer powers of ε',

$h(x,t,\varepsilon') = h_0(x,t)+\varepsilon'h_1(x,t)+...+\varepsilon'^k h_k(x,t)+...,$
whose coefficients are smooth function with bounded norm [29] and they can be found substituting the expansion in the second equation of (9), obtaining [10]

$$\varepsilon'\frac{\partial h}{\partial t} + \varepsilon'\frac{\partial h}{\partial x}\tilde{X}(x,h,t,\varepsilon') = \tilde{Y}(x,h,t,\varepsilon'). \quad (10)$$

B. Application to the histone modification circuit

In order to reduce the system (2), let us first rewrite it by letting $\varepsilon = c\varepsilon'$ and introducing the new time variable $\bar{\tau} = \tau\varepsilon'$:

$$\varepsilon'\frac{d\bar{D}^A}{d\bar{\tau}} = (u_{A0} + u_A + \bar{D}^A)\bar{D} - \varepsilon'(c + \bar{D}^R)\bar{D}^A$$

$$\varepsilon'\frac{d\bar{D}^R}{d\bar{\tau}} = (u_{R0} + u_R + \alpha\bar{D}^R)\bar{D} - \mu'\varepsilon'(cb + \bar{D}^A)\bar{D}^R$$
$$\quad (11)$$
$$\varepsilon'\frac{d\bar{D}}{d\bar{\tau}} = \varepsilon'[\mu(cb + \bar{D}^A)\bar{D}^R + (c + \bar{D}^R)\bar{D}^A]$$

$$\quad - (u_{A0} + u_A + \bar{D}^A + u_{R0} + u_R + \alpha\bar{D}^R)\bar{D}.$$

Furthermore, let us define x, y, f_1 and f_2 as follows:

$$x = \begin{pmatrix} \bar{D}^A \\ \bar{D}^R \end{pmatrix}, \qquad y_2 = \bar{D},$$

$$f_1 = \begin{pmatrix} (u_{A0} + u_A + \bar{D}^A)\bar{D} - \varepsilon'(c + \bar{D}^R)\bar{D}^A \\ (u_{R0} + u_R + \alpha\bar{D}^R)\bar{D} - \mu\varepsilon'(cb + \bar{D}^A)\bar{D}^R \end{pmatrix}, \quad (12)$$
$$f_2 = \varepsilon'[\mu(cb + \bar{D}^A)\bar{D}^R + (c + \bar{D}^R)\bar{D}^A]$$
$$\quad - (u_{A0} + u_A + \bar{D}^A + u_{R0} + u_R + \alpha\bar{D}^R)\bar{D},$$

Now, it is possible to show that $\phi(x)$, defined in **C1**, is equal to 0 and that the matrix A as defined in (4) with $\bar{D} = 0$ and $\varepsilon' = 0$ can be written as

$$\begin{pmatrix} 0 & 0 & (u_A + u_{A0} + \bar{D}^A) \\ 0 & 0 & (u_R + u_{R0} + \alpha\bar{D}^R) \\ 0 & 0 & -(u_A + u_{A0} + \bar{D}^A + u_R + u_{R0} + \alpha\bar{D}^R) \end{pmatrix}. \quad (13)$$

The matrix is singular, showing that the system (11) is a singular singularly perturbed system. More precisely, matrix A has two zero eigenvalues and two corresponding linearly independent eigenvectors. Furthermore, matrix B defined in (5) can be written as

$$B = -(u_A + u_{A0} + \bar{D}^A + u_R + u_{R0} + \alpha\bar{D}^R).$$

When external inputs are not applied ($u_A = u_R = 0$), B has always negative real part if $u_{R0} + u_{A0} \geq l$ with $l > 0$. Then, we can apply Theorem 7.1 from [10] to obtain ε'-dependent the reduced system. Let us first introduce in (11) the change of variable $\tilde{D} = \bar{D}/\varepsilon'$, obtaining

$$\frac{d\bar{D}^A}{d\bar{\tau}} = (u_{A0} + u_A + \bar{D}^A)\tilde{D} - (c + \bar{D}^R)\bar{D}^A$$
$$\frac{d\bar{D}^R}{d\bar{\tau}} = (u_{R0} + u_R + \alpha\bar{D}^R)\tilde{D} - \mu(cb + \bar{D}^A)\bar{D}^R \quad (14)$$
$$\varepsilon'\frac{d\tilde{D}}{d\bar{\tau}} = [\mu(cb + \bar{D}^A)\bar{D}^R + (c + \bar{D}^R)\bar{D}^A]$$
$$\quad - (u_{A0} + u_A + \bar{D}^A + u_{R0} + u_R + \alpha\bar{D}^R)\tilde{D}.$$

To calculate the slow integral manifold from the last equation of (14), let us first construct the asymptotic expansion of $\tilde{D}$:

$$\tilde{D} = h(\bar{D}^A, \bar{D}^R, \varepsilon')$$
$$= h_0(\bar{D}^A, \bar{D}^R) + \varepsilon'h_1(\bar{D}^A, \bar{D}^R) + O(\varepsilon'^2). \quad (15)$$

Then, substituting (15) in the last ODE of (14), we obtain

$$\varepsilon'\frac{dh}{d\bar{\tau}} = \varepsilon'\left(\frac{\partial h}{\partial\bar{D}^A}\frac{d\bar{D}^A}{d\bar{\tau}} + \frac{\partial h}{\partial\bar{D}^R}\frac{d\bar{D}^R}{d\bar{\tau}}\right)$$
$$= [\mu(cb + \bar{D}^A)\bar{D}^R + (c + \bar{D}^R)\bar{D}^A] \quad (16)$$
$$\quad - (u_{A0} + u_A + \bar{D}^A + u_{R0} + u_R + \alpha\bar{D}^R)h.$$

To calculate h_0 and h_1 we equate the terms on the left-hand side and right-hand side multiplied by the same power of ε', obtaining

$$h_0 = \frac{[\mu(cb + \bar{D}^A)\bar{D}^R + (c + \bar{D}^R)\bar{D}^A]}{(u_{A0} + u_A + \bar{D}^A + u_{R0} + u_R + \alpha\bar{D}^R)},$$
$$h_1 = -\frac{\frac{\partial h_0}{\partial\bar{D}^R}((u_{R0} + u_R + \alpha\bar{D}^R)h_0 - \mu(cb + \bar{D}^A)\bar{D}^R)}{(u_{A0} + u_A + \bar{D}^A + u_{R0} + u_R + \alpha\bar{D}^R)}$$
$$\quad (17)$$
$$\quad - \frac{\frac{\partial h_0}{\partial\bar{D}^A}((u_{A0} + u_A + \bar{D}^A)h_0 - (c + \bar{D}^R)\bar{D}^A)}{(u_{A0} + u_A + \bar{D}^A + u_{R0} + u_R + \alpha\bar{D}^R)}.$$

Since $\frac{\partial h_0}{\partial\bar{D}^R}$ and $\frac{\partial h_0}{\partial\bar{D}^A}$ are bounded (and then $\varepsilon'\frac{\partial h_0}{\partial\bar{D}^R}, \varepsilon'\frac{\partial h_0}{\partial\bar{D}^A} \ll 1$ for a sufficiently small ε'), if we substitute (17) into (15) we obtain

$$\tilde{D} = \frac{[\mu(cb + \bar{D}^A)\bar{D}^R + (c + \bar{D}^R)\bar{D}^A]}{(u_{A0} + u_A + \bar{D}^A + u_{R0} + u_R + \alpha\bar{D}^R)}. \quad (18)$$

Substituting (18) into (14) and re-introducing the original time variable $\tau = \bar{\tau}/\varepsilon'$, we finally obtain the reduced system as follows:

$$\frac{d\bar{D}^A}{d\tau} = \left(\frac{\mu(b\varepsilon + \varepsilon'\bar{D}^A)(u_A + \bar{D}^A)}{(u_{A0} + u_A + \bar{D}^A) + (u_{R0} + u_R + \alpha\bar{D}^R)}\right)\bar{D}^R$$
$$\quad - \left(\frac{(\varepsilon + \varepsilon'\bar{D}^R)(u_{R0} + u_R + \alpha\bar{D}^R)}{(u_{A0} + u_A + \bar{D}^A) + (u_{R0} + u_R + \alpha\bar{D}^R)}\right)\bar{D}^A$$
$$\quad (19)$$
$$\frac{d\bar{D}^R}{d\tau} = \left(\frac{(\varepsilon + \varepsilon'\bar{D}^R)(u_{R0} + u_R + \alpha\bar{D}^R)}{(u_{A0} + u_A + \bar{D}^A) + (u_{R0} + u_R + \alpha\bar{D}^R)}\right)\bar{D}^A$$
$$\quad - \left(\frac{\mu(b\varepsilon + \varepsilon'\bar{D}^A)(u_{A0} + u_A + \bar{D}^A)}{(u_{A0} + u_A + \bar{D}^A) + (u_{R0} + u_R + \alpha\bar{D}^R)}\right)\bar{D}^R.$$

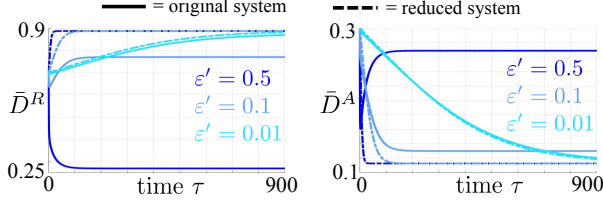**Fig. 2: Trajectories of $\bar{D}^R$ and $\bar{D}^A$ of the original and the reduced system become close as ε' decreases.** Trajectories of $\bar{D}^R$ and $\bar{D}^A$ of the original system (2) (solid lines) and of the reduced system (19) (dashed lines). We set $(\bar{D}^R(0), \bar{D}^A(0)) = (0.7, 0.3)$ as initial conditions and we consider three different values for ε' ($\varepsilon' = 1, 0.1, 0.01$). The values of the other parameters are $u_{A0} = u_{R0} = 0.1$, $u_A = u_R = 0$, $\alpha = b = \mu = c = 1$, $\varepsilon = c\varepsilon'$.

If we sum the ODEs in (19), we obtain $\frac{d\bar{D}^A}{d\tau} + \frac{d\bar{D}^R}{d\tau} = 0$, that is $\bar{D}^A + \bar{D}^R = \text{constant}$. In particular, since $\bar{D}^A + \bar{D}^R + \bar{D} = 1$ and $\bar{D} = \varepsilon'\tilde{D} \approx 0$ for $\varepsilon' \ll 1$, we have that $\bar{D}^A + \bar{D}^R \approx 1$ for $\varepsilon' \ll 1$. We further validated *via* simulation that system (19) is a proper reduction of the original system (2) when ε' is small by showing that the trajectories of $\bar{D}^R$ and $\bar{D}^A$ of the original and reduced systems become closer as ε' decreases (Fig. 2). Multiplying both sides by $D_{tot}(k_E^A D_{tot})$ and defining $\bar{k}_W^A = k_{W0}^A + k_W^A$ and $\bar{k}_W^R = k_{W0}^R + k_W^R$, system (19) can be rewritten in a dimensional form:

$$
\begin{aligned}
\dot{D}^A &= \left(\frac{(\bar{k}_W^A + k_M^A D^A)(\delta + \bar{k}_E^R + k_E^R D^R)}{(\bar{k}_W^A + k_M^A D^A) + (\bar{k}_W^R + k_M^R D^R)} \right) D^R \\
&\quad - \left(\frac{(\bar{k}_W^R + k_M^R D^R)(\delta + \bar{k}_E^A + k_E^A D^A)}{(\bar{k}_W^A + k_M^A D^A) + (\bar{k}_W^R + k_M^R D^R)} \right) D^A \\
\dot{D}^R &= \left(\frac{(\bar{k}_W^R + k_M^R D^R)(\delta + \bar{k}_E^A + k_E^A D^A)}{(\bar{k}_W^A + k_M^A D^A) + (\bar{k}_W^R + k_M^R D^R)} \right) D^A \\
&\quad - \left(\frac{(\bar{k}_W^A + k_M^A D^A)(\delta + \bar{k}_E^R + k_E^R D^R)}{(\bar{k}_W^A + k_M^A D^A) + (\bar{k}_W^R + k_M^R D^R)} \right) D^R.
\end{aligned} \tag{20}
$$

The system is one-dimensional ($D^R + D^A = D_{tot}$) and it can be represented through the following simplified chemical reactions:

$$
\mathrm{D}^A \xrightarrow{k_{AR}} \mathrm{D}^R, \quad \mathrm{D}^R \xrightarrow{k_{RA}} \mathrm{D}^A \tag{21}
$$
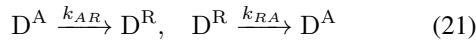
with reaction rate coefficients defined as

$$
\begin{aligned}
k_{AR} &= \left(\frac{(\bar{k}_W^R + k_M^R D^R)(\delta + \bar{k}_E^A + k_E^A D^R)}{(\bar{k}_W^A + k_M^A D^A) + (\bar{k}_W^R + k_M^R D^R)} \right), \\
k_{RA} &= \left(\frac{(\bar{k}_W^A + k_M^A D^A)(\delta + \bar{k}_E^R + k_E^R D^A)}{(\bar{k}_W^A + k_M^A D^A) + (\bar{k}_W^R + k_M^R D^R)} \right).
\end{aligned} \tag{22}
$$

A diagram of the circuit is shown in Fig. 3.

IV. STOCHASTIC ANALYSIS

The reduced chemical reaction system (21) can be represented by a one-dimensional Markov chain in which the state x represents the number of D^R, that
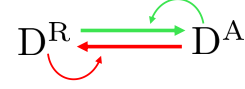

Fig. 3: Reduced histone modification circuit. Diagram of the circuit reactions in (21). The green arrows correspond to the first reaction in (21) and the red arrows correspond to the second reaction in (21). Since the reaction rate constants, defined in (22), increase with the concentration of the reaction product, we have two autocatalytic loops, highlighted by the thin arrows.

is, $x = n_{D^R}$ with $x \in [0, D_{tot}]$. Furthermore, given a generic state x, the rate associated to the transition from x to $x+1$, α_x, and the rate associated to the transition from x to $x-1$, γ_x, can be written as

$$
\begin{aligned}
\alpha_x &= \left(\frac{(\bar{k}_W^R + \frac{k_M^R}{\Omega}x)(\varepsilon + \varepsilon'\frac{x}{D_{tot}})}{(\bar{u}_A + \frac{(D_{tot}-x)}{D_{tot}}) + (\bar{u}_R + \alpha\frac{x}{D_{tot}})} \right) (D_{tot} - x), \\
\gamma_x &= \left(\frac{(\bar{k}_W^A + \frac{k_M^A}{\Omega}(D_{tot} - x))\mu(b\varepsilon + \varepsilon'\frac{(D_{tot}-x)}{D_{tot}})}{(\bar{u}_A + \frac{(D_{tot}-x)}{D_{tot}}) + (\bar{u}_R + \alpha\frac{x}{D_{tot}})} \right) x.
\end{aligned} \tag{23}
$$

Now, we want to determine how the circuit parameters affect the duration of the memory of chromatin states. Let us first analytically evaluate the stationary probability distribution $\pi(x)$. Since this Markov chain is irreducible and reversible, we can obtain an analytical expression for $\pi(x)$ by applying detailed balance [11]. In particular, for our one-dimensional Markov chain, the detailed balance principle allows us to write the stationary distribution $\pi(x)$ as

$$
\pi(x) = \prod_{i=1}^{x} \frac{\alpha_{x-1}}{\gamma_x} \pi(0) = \frac{\prod_{i=1}^{x} \frac{\alpha_{x-1}}{\gamma_x}}{\left(1 + \sum_{j=1}^{D_{tot}} \left(\prod_{i=1}^{j} \frac{\alpha_{x-1}}{\gamma_x} \right) \right)} \tag{24}
$$

for any $x \in [1, D_{tot}]$. Since $\prod_{i=1}^{x} \frac{\alpha_{x-1}}{\gamma_x} = O(\varepsilon)$ for any $x \geq 1$ except for $x = D_{tot}$, for $\varepsilon \to 0$ the stationary probability distribution $\pi(x)$ can be approximated by

$$
\lim_{\varepsilon \to 0} \pi(x) = \pi_0(x) = \begin{cases} \frac{1}{1+P} & \text{if } x = 0 \\ 0 & \text{if } x \neq 0, D_{tot} \\ \frac{P}{1+P} & \text{if } x = D_{tot} \end{cases} \tag{25}
$$

with

$$
P = \frac{(\bar{u}_A + \bar{u}_R + \alpha)(\bar{u}_R)}{(\bar{u}_A + \bar{u}_R + 1)(\bar{u}_A)b} \prod_{i=1}^{D_{tot}-1} \left(\frac{\bar{u}_R + \alpha\frac{i}{D_{tot}}}{\bar{u}_A + \frac{D_{tot}-i}{D_{tot}}} \right) \left(\frac{1}{\mu} \right)^{D_{tot}}, \tag{26}
$$

in which $\bar{u}_A = u_{A0} + u_A$, $\bar{u}_R = u_{R0} + u_R$. From (25), we note that as ε tends to zero, $\pi(x) \to 0$ for all x except for $x = D_{tot}$ (fully repressed chromatin state) and $x = 0$ (fully active chromatin state), that is, the distribution has two modes in correspondence of $x = 0$
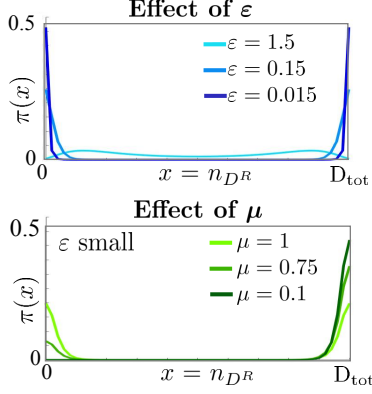
Fig. 4: Effect of key parameters on the stationary probability distribution of the histone modification circuit. The stationary distribution of the circuit related to reactions (21) obtained analytically, (24). The variable $x \in [0, \mathrm{D_{tot}}]$ represents the number of nucleosomes characterized by repressive histone marks, n_{D^R}, with $x = \mathrm{D_{tot}}$ corresponding to the fully repressed chromatin state and with $x = 0$ corresponding to the fully active chromatin state. In the graphs we show how the stationary distribution is affected by ε (upper side) and μ (lower side). The parameter values of each regime are listed in Table I.

and $x = \mathrm{D_{tot}}$, and the probability of having the system in the intermediate states tends to zero (Fig. 4). This suggests that when $\varepsilon \to 0$, a system starting at $x = \mathrm{D_{tot}}$ or at $x = 0$ will remain at that state. Qualitatively, this indicates that ε small allows to keep the memory of the repressed or active chromatin state for very long time, suggesting that ε controls ECM.

In order to make this statement mathematically precise, we evaluate how the system parameters affect the temporal duration of the memory of the fully repressed ($x = \mathrm{D_{tot}}$) and fully active ($x = 0$) chromatin states. More precisely, defining the hitting time of $x = j$ starting from $x = i$ as $t_i^j := [\inf\{t \geq 0 : x(t) = j$ with $x(0) = i\}$ with $i, j \in [0, \mathrm{D_{tot}}]]$, the time to memory loss of the fully repressed chromatin state can be defined as $\tau_{\mathrm{D_{tot}}}^0 = \mathbb{E}(t_{\mathrm{D_{tot}}}^0)$. Similarly, we can define the time to memory loss of the active state as the expected value of the first time at which the $x = \mathrm{D_{tot}}$, starting from $x = 0$, that is $\tau_0^{\mathrm{D_{tot}}} = \mathbb{E}(t_0^{\mathrm{D_{tot}}})$. In order to compute $\tau_{\mathrm{D_{tot}}}^0$ and $\tau_0^{\mathrm{D_{tot}}}$ we use first step analysis [12]. Given the definition of α_x and γ_x in (23), the time to memory loss of the repressed chromatin state, $\tau_{\mathrm{D_{tot}}}^0$, can be written as follows:

$$
\tau_{\mathrm{D_{tot}}}^0 = \frac{r_{\mathrm{D_{tot}}-1}}{\gamma_{\mathrm{D_{tot}}}} \left(1 + \sum_{x=1}^{\mathrm{D_{tot}}-1} \frac{1}{r_x} \right) + \frac{1}{\gamma_1}
$$
$$
+ \sum_{x=2}^{\mathrm{D_{tot}}-1} \left[\frac{r_{x-1}}{\gamma_x} \left(1 + \sum_{j=1}^{x-1} \frac{1}{r_j} \right) \right], \tag{27}
$$

with $r_x = \frac{\alpha_1 \alpha_2 \ldots \alpha_x}{\gamma_1 \gamma_2 \ldots \gamma_x}$. Assuming $\varepsilon' \neq 0$, the dominant term of $\tau_{\mathrm{D_{tot}}}^0$ for $\varepsilon \ll 1$ is the first addend in (27). Then, by normalizing the time to memory loss with respect $\frac{k_M^A \mathrm{D_{tot}}}{\Omega}$ ($\bar{\tau}_{\mathrm{D_{tot}}}^0 = \tau_{\mathrm{D_{tot}}}^0 \frac{k_M^A \mathrm{D_{tot}}}{\Omega}$), the normalized $\tau_{\mathrm{D_{tot}}}^0$ in the regime $\varepsilon \ll 1$ can be approximated as follows:

$$
\bar{\tau}_{\mathrm{D_{tot}}}^0 \approx \frac{K_R}{\mu \varepsilon} \left(1 + \sum_{x=1}^{\mathrm{D_{tot}}-1} \frac{K_R^x}{h_1^x(\mu)} \right), \tag{28}
$$

with h_1^x an increasing function, $h_1^x(0) = 0$ and K_R and K_R^x functions independent of ε and μ. In a similar way, we can determine the time to memory loss of the active gene state, $\tau_0^{\mathrm{D_{tot}}}$, that can be written as follows:

$$
\tau_0^{\mathrm{D_{tot}}} = \frac{\tilde{r}_{\mathrm{D_{tot}}-1}}{\alpha_0} \left(1 + \sum_{x=1}^{\mathrm{D_{tot}}-1} \frac{1}{\tilde{r}_x} \right) + \frac{1}{\alpha_{\mathrm{D_{tot}}-1}}
$$
$$
+ \sum_{x=2}^{\mathrm{D_{tot}}-1} \left[\frac{\tilde{r}_{x-1}}{\alpha_{\mathrm{D_{tot}}-x}} \left(1 + \sum_{j=1}^{x-1} \frac{1}{\tilde{r}_j} \right) \right], \tag{29}
$$

with $\tilde{r}_x = \frac{\gamma_{\mathrm{D_{tot}}-1} \gamma_{\mathrm{D_{tot}}-2} \ldots \gamma_{\mathrm{D_{tot}}-x}}{\alpha_{\mathrm{D_{tot}}-1} \alpha_{\mathrm{D_{tot}}-2} \ldots \alpha_{\mathrm{D_{tot}}-x}}$. Also in this case, assuming that $\varepsilon' \neq 0$, the dominant term of $\tau_0^{\mathrm{D_{tot}}}$ for $\varepsilon \ll 1$ is the first addend in (29). Then, by normalizing the time to memory loss with respect $\frac{k_M^A \mathrm{D_{tot}}}{\Omega}$ ($\bar{\tau}_0^{\mathrm{D_{tot}}} = \tau_0^{\mathrm{D_{tot}}} \frac{k_M^A \mathrm{D_{tot}}}{\Omega}$), the normalized $\tau_0^{\mathrm{D_{tot}}}$ in the regime $\varepsilon \ll 1$ can be approximated as follows:

$$
\bar{\tau}_0^{\mathrm{D_{tot}}} \approx \frac{K_A}{\varepsilon} \left(1 + \sum_{x=1}^{\mathrm{D_{tot}}-1} \frac{h_2^x(\mu)}{K_A^x} \right), \tag{30}
$$

with h_2^x an increasing function, $h_2^x(0) = 0$ and K_A and K_A^x functions independent of ε and μ. In the limiting condition $\varepsilon \to 0$, we have that both $\bar{\tau}_{\mathrm{D_{tot}}}^0$ and $\bar{\tau}_0^{\mathrm{D_{tot}}}$ tend to infinity. Therefore, a lower ε is the driver of longer lasting memory of both the active and repressed chromatin states.

Now, let us also determine how μ, the non-dimensional parameter quantifying the asymmetry between the erasure rates of repressive and activating modifications, affects the ECM. From the expression of the stationary distribution in (25), it is possible to notice that if μ is decreased, $\pi_0(\mathrm{D_{tot}})$ increases to the detriment of $\pi_0(0)$, that is the stationary distribution is biased towards the repressed state (Fig. 4). *Viceversa* if μ is increased. In accordance with this result, a lower μ leads to higher $\bar{\tau}_{\mathrm{D_{tot}}}^0$ but to lower $\bar{\tau}_0^{\mathrm{D_{tot}}}$.

V. SIMULATION RESULTS

In the previous section we exploited a deterministic quasi-steady state approximation [33] to derive the reduced chemical reaction system (21). In general there is no proof that a reduced reaction system obtained by using a deterministic quasi-steady state approximation is a good approximation of the original reaction system.
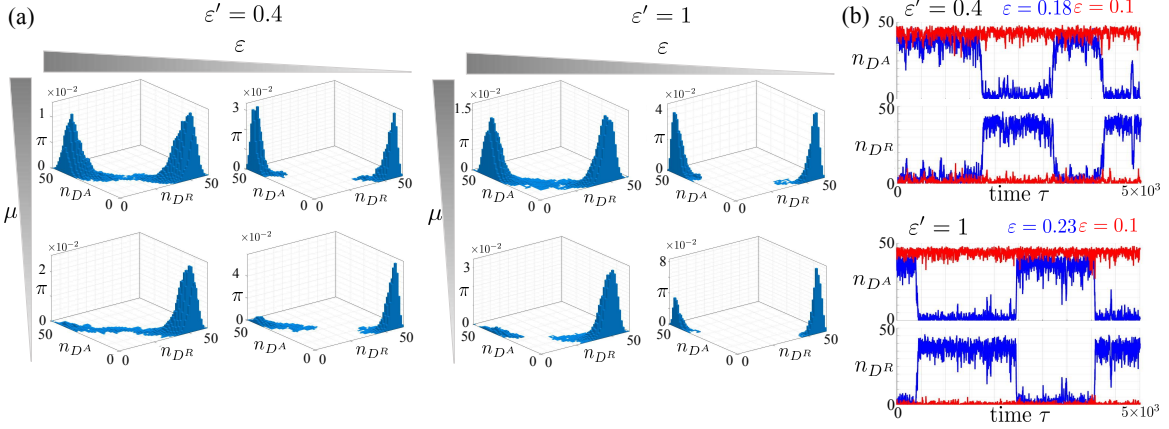
Fig. 5: Stochastic simulations of the histone modification circuit in Fig. 1(a) using SSA. (a) The stationary distribution for the histone modification circuit whose reactions are listed in Fig. 1(a). The parameter values are in Table II. In particular, in the left-side plots $\varepsilon = 0.18, 0.1$, $\mu = 1, 0.8$ and $\varepsilon' = 0.4$ and in the right-side plots $\varepsilon = 0.23, 0.1$, $\mu = 1, 0.8$ and $\varepsilon' = 1$. In all plots n_{D^A} and n_{D^R} represent the number of nucleosomes with active histone marks and repressive histone marks, respectively. (b) Time trajectories of n_{D^A} and n_{D^R} starting from the fully active state $n_{D^A} = 50$, $n_{D^R} = 0$ for different values of ε and ε'. The time is normalized ($\tau = t\frac{k_M^A}{\Omega}D_{\mathrm{tot}}$, with Ω the reaction volume) and the parameter values are in Table II.

However, we were interested in exploiting the one-dimensional reduced model to analytically determine the trends with which the key parameters affect the system behavior. This is the reason why here we perform computational study of the original system in reactions of Fig. 1(a) by using the Stochastic Simulation Algorithm (SSA) [13] (Fig. 5) to illustrate that the analytically derived trends are accordance with the results obtained by simulations of the original model of chemical reaction. The trend with which ε and μ affect the stationary distribution is in accordance with what we determine by studying the analytical expressions of $\pi(x)$ (24) (Fig. 5(a)). Furthermore, the time trajectories in Fig. 5(b) show less frequent transitions between the active and repressed chromatin states for lower values of ε, in agreement with the mathematical expression of the time to memory loss expressions (28),(30).

VI. CONCLUSION

In this work, a ubiquitous circuit motif among histone modifications [9] has been considered. In order to study the extent of memory of the active and repressed chromatin states, a time scale separation between erasure reactions and autocatalytic reactions has been exploited to obtain a one-dimensional reduced model. The advantage of using this model reduction approch was that it allowed us to analytically determine both the stationary distribution of the system and an expression for the time to memory loss, and to analyze in a simple, but rigorous way, the trends with which the circuit parameters affect them. Concerning the stationary distribution, for a sufficiently small ε the analysis shows two concentrated peaks in the active and repressed chromatin states. More

Param.	Value upper plot	Value lower plot	Param.	Value upper plot	Value lower plot
u_{A0}	0.1	0.1	ε	1.5,0.15,0.015	0.1
u_A	0	0	ε'	0.1	0.1
u_{R0}	0.1	0.1	b	1	1
u_R	0	0	μ	1	1, 0.8, 0.1
α	1	1	D_{tot}	50	50

TABLE I: Parameter values relative to the plots in Fig.4.

Param.	Value (h^{-1}) Fig.5(a) left plots	Value (h^{-1}) Fig.5(a) right plots	Value (h^{-1}) Fig.5(b) upper plots	Value (h^{-1}) Fig.5(b) lower plots
k_{w0}^A	5	5	5	5
k^A	0	0	0	0
k_{w0}^R	5	5	5	5
k_w^R	0	0	0	0
k_M^A/Ω	1	1	1	1
δ	4.3,2.5	5.7,2.5	4.3,2.5	5.7,2.5
$\bar{k}_E^A$	4.3,2.5	5.7,2.5	4.3,2.5	5.7,2.5
k_E^A/Ω	0.4	1	0.4	1
k_M^R/Ω	1	1	1	1
$\bar{k}_E^R$	4.3,2.5 (up. plots) 3.44,2(low. plots)	5.7,2.5 (up.plots) 4.56,2(low. plots)	4.3,2.5	5.7,2.5
k_E^R/Ω	0.4,0.32	1,0.8	0.4	1

TABLE II: Parameter values relative to the plots in Fig.5.

precisely, the smaller ε is, the more concentrated the peaks are until, for $\varepsilon \to 0$, $\pi(x) \neq 0$ only in correspondence of the fully active state ($n_{D^A} = D_{\mathrm{tot}}$) and fully repressed state ($n_{D^R} = D_{\mathrm{tot}}$). Furthermore, the height of the peaks depends on the value of μ. Specifically, high μ shifts the distribution towards the active state to the detriment of the repressed state (*viceversa* for low μ). These results are consistent with the analysis of the time to memory loss, that shows longer memory of the active and repressed states for smaller values of ε.

Furthermore, a lower value of μ increases the memory of the repressed state, while decreases the memory of the active state. These results are in agreement with the simulations conducted for the original reaction system (Fig. 1(a)) with the SSA. Future work will investigate the stochastic behavior of the chromatin modification circuit that includes also DNA methylation.

REFERENCES

[1] J. Holmberg and T. Perlmann, "Maintaining differentiated cellular identity," *Nature Reviews*, vol. 13, 2012.

[2] M. Ptashne, "Epigenetics: Core misconcept," *Proc. Natl. Acad. Sci*, vol. 110, 2013.

[3] W. Xiong and J. E. F. Jr, "A positive-feedback-based bistable 'memory module' that governs a cell fate decision," *Nature*, vol. 426, 2003.

[4] J. X. Zhou and S. Huang, "Understanding gene circuits at cell-fate branch points for rational cell reprogramming," *Trends in Genetics, Cell*, vol. 27, pp. 55–62, 2011.

[5] C. Furusawa and K. Kaneko, "A dynamical-systems view of stem cell biology," *Science*, vol. 338, 2012.

[6] C. Furusawa and K. Kaneko, "Bistability, bifurcations, and waddington?s epigenetic landscape," *Current Biology*, vol. 22, 2012.

[7] N. Carey, *The epigenetic revolution*. Columbia University Press, 2013.

[8] C. D. Allis, M.-L. Caparros, T. Jenuwein, and D. Reinberg, *Epigenetics*. Cold Spring Harbor Laboratory Press, Second Edition, 2015.

[9] I. B. Dodd, M. A. Micheelsen, K. Sneppen, and G. Thon, "Theoretical analysis of epigenetic cell memory by nucleosome modification," *Cell*, vol. 129, 2007.

[10] V. Sobolev, *7. Geometry of Singular Perturbations: Critical Cases*. SIAM, 2005.

[11] C. W. Gardiner, *Handbook of stochastic methods for physics, chemistry and the natural sciences*. Springer-Verlag, 1994.

[12] J. R. Norris, *Markov Chains*. Cambridge University Press, 1997.

[13] D. T. Gillespie, "Stochastic simulation of chemical kinetics," *Annual Review of Physical Chemistry*, 2007.

[14] S. Berry, C. Dean, and M. Howard, "Slow chromatin dynamics allow polycomb target genes to filter fluctuations in transcription factor activity," *Cell Systems*, vol. 4, 2017.

[15] S. Mukhopadhyay and A. M. Sengupta, "The role of multiple marks in epigenetic silencing and the emergence of a stable bivalent chromatin state," *PLOS Comput. Biol.*, vol. 0, 2012.

[16] I. B. Dodd and K. Sneppen, "Barriers and silencers: A theoretical toolkit for control and containment of nucleosome-based epigenetic states," *J. Mol. Biol.*, vol. 414, 2011.

[17] M. Sedighi and A. M. Sengupta, "Epigenetic chromatin silencing: bistability and front propagation," *Phys. Biol.*, vol. 4, 2007.

[18] K. Sneppen and I. B. Dodd, "A simple histone code opens many paths to epigenetics," *PLOS Comput. Biol.*, 2012.

[19] H. Zhang, X.-J. Tian, A. Mukhopadhyay, K. S. Kim, and J. Xing, "Statistical mechanics model for the dynamics of collective epigenetic histone modification," *PHYSICAL REVIEW LETTERS*, vol. 114, 2014.

[20] D. D. Vecchio and R. M. Murray, *Biomolecular Feedback Systems*. Princeton University Press, 2014.

[21] N. A. Hathaway, O. Bell, C. Hodges, E. L. Miller, D. S. Neel, and G. R. Crabtree, "Dynamics and memory of heterochromatin in living cells," *Cell*, vol. 149, 2012.

[22] M. Trerotola, V. Relli, P. Simeone, and S. Alberti, "Epigenetic inheritance and the missing heritability," *Human Genomics*, vol. 9, 2015.

[23] T. Zhang, S. Cooper, and N. Brockdorff, "The interplay of histone modifications – writers that read," *EMBO Reports*, 2015.

[24] E. I. Campos, J. M. Stafford, and D. Reinberg, "Epigenetic inheritance: Histone bookmarks across generations," *Trends Cell Biol*, vol. 24, 2014.

[25] C. Alabert, T. K. Barth, N. Reveron-Gomez, S. Sidoli, A. Schmidt, O. N. Jensen, A. Imhof, and A. Groth, "Two distinct modes for propagation of histone ptms across the cell cycle," *Research Communication, CSHL*, 2015.

[26] S. Huang, M. Litt, and C. A. Blakey, *Epigenetic Gene Expression and Regulation*. Academic Press, 2015.

[27] L. Bintu, J. Yong, Y. E. Antebi, K. McCue, Y. Kazuki, N. Uno, M. Oshimura, and M. B. Elowitz, "Dynamics of epigenetic regulation at the single-cell level," *Science*, 2016.

[28] S. Wiggins, *Introduction to Applied Nonlinear Dynamical Systems and Chaos*. 2ed., Springer, 2003.

[29] M. P. M. E. Shchepakina. V. Sobolev, *Singular Singularly Perturbed Systems*. Springer, 2014.

[30] S. V. Kononenco L.I., "Asymptotic decomposition of slow integral manifolds," *Siberian Mathematical Journal*, vol. 35, 1994.

[31] V. Sobolev, "Integral manifolds and decomposition of singularly perturbed systems," *Systems & Control Letters*, vol. 5, 1984.

[32] D. Henry, *Geometric Theory of Semilinear Parabolic Equations*. Springer, Berlin, Heidelberg, 1981.

[33] J. K. Kim, K. Josić, and M. R. Bennett, "The validity of quasi-steady-state approximations in discrete stochastic simulations," *Biophysical Journal*, vol. 107, no. 3, pp. 783–793, 2014.